Direct optical micropatterning of poly(dimethylsiloxane) for microfluidic devices

Shaorui Gao,[1] Wing-Tai Tung,[1] Dexter Siu-Hong Wong,[2] Liming Bian[2] and A. Ping Zhang*[1]

[1]Photonics Research Centre, Department of Electrical Engineering, The Hong Kong Polytechnic University, Hong Kong SAR, China
[2]Division of Biomedical Engineering, Department of Mechanical and Automation Engineering, The Chinese University of Hong Kong, Hong Kong SAR, China

*E-mail: azhang@polyu.edu.hk

Abstract

Poly(dimethylsiloxane) (PDMS) is one of the most popular polymer materials for microfluidic devices. However, it still remains a challenge to rapidly fabricate PDMS microfluidic devices with micrometer-scale feature sizes. In this paper, we present a gray-scale digital photolithography technology for direct patterning of large-area high-resolution PDMS microstructures for biomicrofluidic applications. With the positive- and negative-tone photosensitive PDMS (photoPDMS), we rapidly fabricated various PDMS microstructures with complex geometries by using an one-step patterning process. The positive-tone PDMS has been used to pattern large-area microfluidic chips, while the negative-tone PDMS has been utilized to fabricate high-resolution on-chip microstructures and components. In particular, a large-area microfluidic chip of 5.5 × 2.8 cm^2 with complex three-dimensional (3D) staggered herringbone mixers (SHMs) was fabricated from the positive-tone PDMS by using a single-step optical exposure process; a small microfluidic chip with feature size as small as 5 μm was prepared with the negative-tone PDMS. Furthermore, 3D surface engineering of PDMS microchannels was demonstrated to customize extracellular microenvironments for investigating cell migration.

Keywords: Digital photolithography, poly(dimethylsiloxane), microfluidic devices, cell migration

1. Introduction

Microfluidics enables integration of a large number of components for multiple functions on a single small chip, such as fluidic flow or droplet control, microparticle or cell manipulation and biochemical analysis. Due to the scaling down of size, microfluidics offers numerous advantages, including large surface-to-volume ratio, ease of sample handling, fast sample separation and detection, and reduced consumption of both energy and reagents. Although microfluidic chip can be fabricated in different materials, e.g., silicon and glass [1, 2], soft polymer materials have become most common because of their ease of fabrication, excellent chemical and physical properties as well as biocompatibility [3].

Poly(dimethylsiloxane) (PDMS) has become one of the most popular candidates for fabrication of microfluidic devices. This is attributed to its own distinctive advantages: firstly, the technical features such as high-fidelity replication and ease of handling; secondly, the excellent material properties, including nontoxic, electrically insulating, optically transparent and chemical inertness [4]. The well-known fabrication method for PDMS microfluidic chips is the soft lithography [5, 6], which is a combination of printing, moulding and embossing processes with an elastomeric template. A master mold made of photoresist is commonly prepared by photolithographic processes with a photomask [7] or maskless exposure techniques [8-10].

Since the preparation of a master is time consuming and costly, one of growing demands is to discard the replication procedure to simplify the overall process of PDMS microstructures. It has been demonstrated that PDMS microfluidic chips can be directly prepared by using photolithographic processes with a photomask via photolytic degradation of pre-cured PDMS [11], photo-inhibition assisted thermal-crosslinking [12, 13] and photo-crosslinking of liquid photosensitive PDMS (photoPDMS) [13-15].

However, the use of photomask in conventional photolithography will also induce some limitations, such as long lead-time and limited early prototyping, and is not applicable to adaptive fabrications. In order to overcome those problems, D. Lu et al.[16] proposed to use femtosecond laser direct writing to fabricate PDMS microstructures and devices. However, such a technique is less productive, which is mainly attributed to their single-spot scanning manner. An alternative method demonstrated by T. Femmer et al.[17] is to use a digital-micromirror-device (DMD) based commercial 3D printer to directly print PDMS devices. Despite its one-step fabrication processing ability, such a technique has relatively large feature size between 150 and 300 μm and thus not suitable to fabricate high-resolution microfluidic chips whose typical channel sizes are of tens of micrometers or even smaller.

Here, we present another DMD-based optical processing technology, called gray-scale digital photolithography (gDPL), to fabricate high-resolution PDMS devices, as shown in Fig. 1. Two kinds of photoPDMS materials, i.e. positive- and negative-tone photoPDMS, are used to fabricate various PDMS microstructures and microfluidic devices. In addition to dynamic optical exposure capabilities that we demonstrated to 3D patterning of hydrogels [18, 19] and SU-8 photoresist [20],

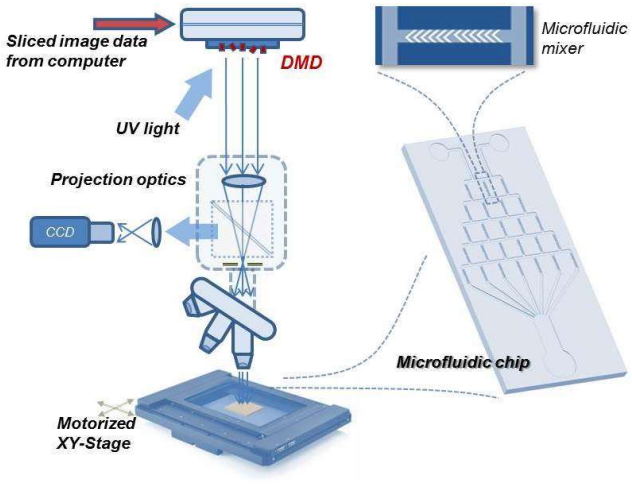

Fig. 1 Schematic diagram of the gray-scale digital photolithography setup for direct micropatterning of PDMS microstructures for microfluidic devices.

a multiscale optical patterning process is demonstrated to fabricate a large-area microfluidic chip by using the positive-tone photoPDMS (P-photoPDMS) and then additively print ultrafine on-channel microstructures by using the negative-tone photoPDMS (N-photoPDMS).

2. Materials and methods

2.1 Gray-scale digital photolithography setup

A gDPL setup, as depicted in Fig. 1, is developed via integrating a DMD chip (DLi4120 0.7 XGA, DLP Texas Instruments) with a high-power UV light source (whose wavelength is 365 nm; OmniCure 2000 System, Lumen Dynamic Group Inc.), a set of projection optics with three different objective lenses (M-set, Newport) and a high-precision motorized XY-stage (whose resolution is 0.1 μm; M-687 PILine, Physik Instrumente). The DMD chip acts as a high-speed dynamic virtual mask and generates optical patterns according to an image flow from a computer in real time. The objective lenses are configurable for multi-scale optical exposure processes. A seamless pattern stitching technique has been developed to overcome the size limitation of a single DMD chip to enable the fabrication of large-area microfluidic devices.

2.2 Preparation of positive and negative photosensitive PDMS

PDMS base, curing agent and benzophenone were used to prepare the P-photoPDMS [12]. Firstly, the PDMS base and the curing agent (Sylgard® 184 Silicone Elastomer kit, Dow Corning) were fully mixed in the ratio of 10 : 1 (m/m). Benzophenone (Sigma-Aldrich) was fully dissolved in xylene and then was mixed with the PDMS mixture for 30 min. Different mixture ratios (0.25 wt%, 0.5 wt%, and 0.75 wt%, respectively) were used in the experiments, while the ratio of xylene and PDMS mixture kept unchanged as 15 wt%. The mixture was then degassed for 30 min to completely remove air bubbles. The PDMS base monomer is vinyl terminated, while the crosslinker is methyl terminated due to its silicon hydride groups. During curing process, the reaction between the monomer's vinyl groups and the crosslinker's silicon hydride groups makes PDMS monomers crosslinked. Upon UV exposure (at the wavelength of 365 nm), benzophenone generates radicals, which can react with the silicon hydride groups of the crosslinker and then inhibit crosslinking reaction. After post-exposure baking, the unexposed PDMS becomes cured, while in the exposure region PDMS monomer remains uncured and can be washed away by xylene.

The N-photoPDMS contains PDMS copolymer VDT 954 (Gelest Inc.) and 2,2-dimethoxy-2-phenyl acetophenone [15]. VDT 954 was firstly dissolved in methyl isobutyl ketone (MIBK, Sigma-Aldrich) in the ratio of 6 : 4 (m/m), and then 2,2-dimethoxy-2-phenyl acetophenone (Igracure 651, Ciba Specialty Chemicals Inc.) was added as photoinitiator. Different ratios (1 wt%, 3 wt%, and 5 wt%, respectively) of Igracure 651 and VDT 954 were used in the experiments. The mixture was fully mixed for 1 hour and degassed for 30 min. Upon UV exposure (at the wavelength of 365 nm), the photoinitiator Igracure 651 generates free radicals, which initiate the crosslinking of VDT 954 with vinyl group. The unexposed PDMS region remains uncrosslinked and can be washed away using a mixture of MIBK and isopropanol (1:1, v/v).

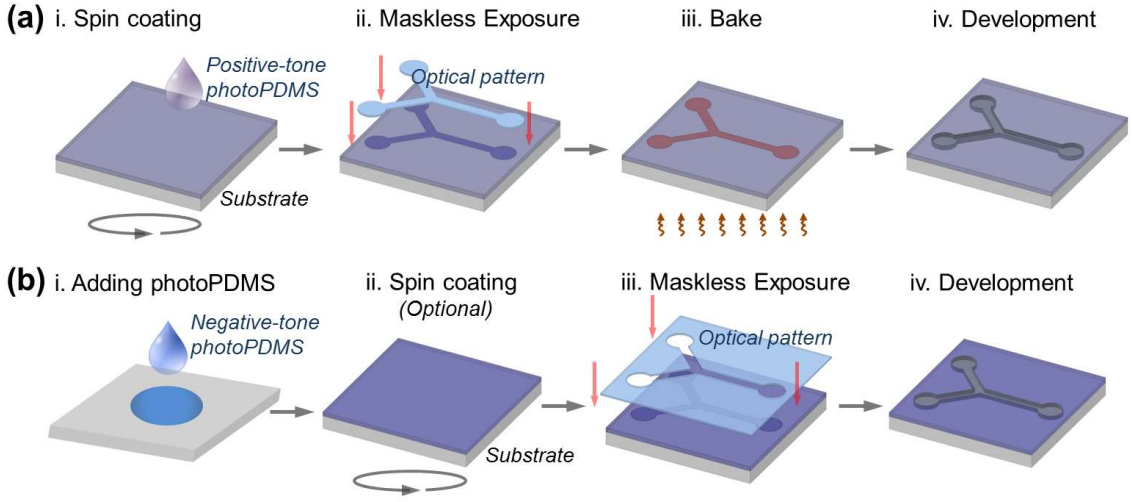

Fig. 2 Schematic diagrams of the processing flows of direct optical micropatterning of PDMS micropatterns and devices with (a) positive-tone photoPDMS and (b) negative-tone photoPDMS, respectively.

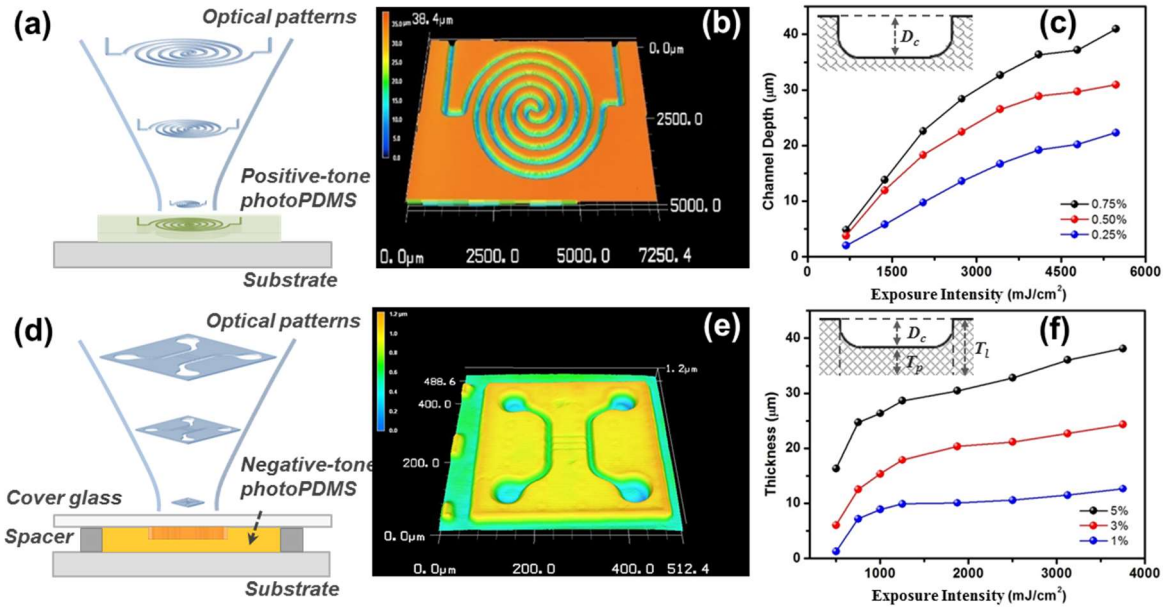

Fig. 3 Micropatterning of PDMS microchannels: (a) schematic of the top-down exposure process for P-photoPDMS, (b) the laser scanning confocal image of a 5-loop double spiral microfluidic device, (c) the dependency of the P-photoPDMS microchannel's depth the on the exposure intensity, (d) schematic of the bottom-up exposure process for N-photoPDMS, (e) the laser scanning confocal image of a small microfluidic chip with 5-μm-wide connecting channels, (f) the dependency of the N-photoPDMS microchannel's depth the on the exposure intensity.

2.3 Fabrication processes

The fabrication of high-resolution PDMS devices involves: spin coating, optical exposure, bake and development, as shown in Fig. 2(a) and (b). To fabricate P-photoPDMS devices, the prepared mixture was firstly spin-coated on a 1-mm-thick glass substrate (e.g. 1″× 1″) at the spin rate ranging from 700 rpm to 3000 rpm (depending on the desired thickness) for 30 seconds. The P-photoPDMS coated substrate was then placed under the gDPL setup for optical maskless exposure. The 3D model of PDMS device was designed by using commercial CAD software, and an own-developed add-on program was used to slice the model into a series of images with ~200 layers. Images were then sequentially uploaded to the DMD chip to dynamically generate optical patterns. Owing to the additive penetration depth of UV light, P-photoPDMS microstructures with complex profiles can then be fabricated via precise control of exposure time, which typically ranges from several seconds to tens of seconds. Following the optical exposure process, a post-exposure bake was conducted on a hotplate at 85 °C for 3 ~ 5 minutes (depending on the thickness of the PDMS film). Finally, the sample was immersed into the MIBK and isopropanol (1:1, v/v) solution for 1 hour for complete development, and then rinsed with isopropanol and dried with nitrogen gas. To fabricate N-photoPDMS microstructures, the fabrication processes are very similar to that of the P-photoPDMS, except the eliding of post-exposure bake. It is because N-photoPDMS gets cured during optical exposure process.

3. Results and discussion

3.1 Direct micropatterning of PDMS microstructures

With P-photoPDMS and N-photoPDMS, diverse PDMS microstructures can be rapidly patterned by using the gDPL technology. Fig. 3(a) depicts the schematic of the top-down exposure process using P-photoPDMS. Because of its positive-acting property, the exposed regions of P-photoPDMS consequently become notched after development. Fig. 3(b) shows a 5-loop double spiral microfluidic device, whose size, channel width and height are 7.2 × 5.0 mm², 250 μm and 28 μm, respectively, which have potential applications in filtration [21] and mixing [22]. More examples of the fabricated P-photoPDMS microstructures, e.g. flower-like microstructure array, are shown in Fig. 4.

The dependency of the depth of channel on the exposure intensity of UV light is presented on Fig. 3(c). The width of the optical pattern is 100 μm, and the UV intensity is 330 mW/cm², while the exposure time ranges from 2 to 16 seconds with an interval of 2 seconds. One can see that deeper microfluidic channel can be formed with the increment of exposure intensity because more radicals are generated to react with the curing agent. The depth of channel can reach up to 40 μm when the concentration of benzophenone is 0.75 wt% and the exposure energy is ~ 5300 mJ/cm². Although higher concentration of benzophenone can produce deeper channel, experimental results revealed that excess benzophenone will cause

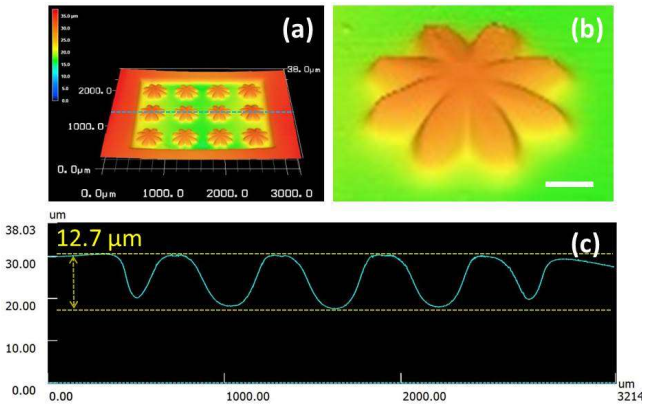

Fig. 4 Laser-scanning confocal images of the fabricated flower-like microstructures using P-photoPDMS. (a) confocal image of the PDMS structure, (b) enlarged image of a flower-like microstructure, scale bar: 100 μm, (c) a cross-section profile of the PDMS microstructure.

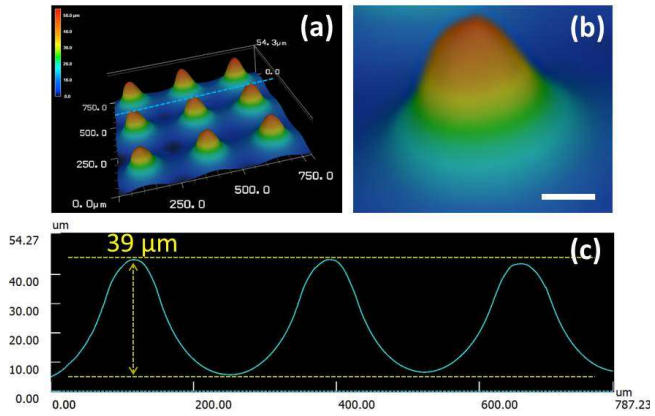

Fig. 5 Laser-scanning confocal images of the fabricated micro-cone array using N-photoPDMS. (a) confocal image of the micro-cone array, (b) enlarged image of a micro-cone, scale bar: 100 µm, (c) a cross-section profile of the micro-cone array.

crystallization of the mixture shortly after the spin-coating when the concentration of benzophenone reaches 0.75 wt%, and then results in a degradation of the surface quality of the sample. It is noteworthy that the increment of the channel depth will eventually come to an end according to the Beer-Lambert law because UV light gets weaker with the penetration in PDMS.

To fabricate N-photoPDMS microstructures, the spin-coated PDMS film is typically inversely placed with spacers for optical exposure process, as depicted in Fig. 3(d), and UV-transparent glass substrates are commonly used in the experiments. Fig. 3(e) shows a fabricated small microfluidic chip with the size of 450 × 450 µm^2. One can see that two main channels with width of 20 µm were fabricated and another three connecting channels with the width of 5 µm were successfully generated. More examples of N-photoPDMS microstructures are presented in Fig. 5. It is noteworthy that PDMS microstructures with sharp edge can be fabricated by the technology with N-photoPDMS. Fig. S1 shows a fabricated PDMS micro-ring structure. One can see from the cross-section profile of the microstructure that the sharp edge with sidewall angle up to 86 degree was fabricated. Such a result indicates that the technology can be used to fabricate PDMS microfluidic devices with clear edge definition.

If N-photoPDMS is used to fabricate micro-channels, the region outside the channel needs fully exposed, while the channel region keeps unexposed. Fig. 3(f) shows the dependence of the thickness of the cured N-photoPDMS on the exposure energies when the photoinitiator concentrations are 1 wt%, 3 wt% and 5 wt%, respectively. As depicted in the inset in Fig. 3(f), if assume that the thickness (T_l) of the spin-coated layer is fixed, the channel depth (D_c) is determined by the thickness (T_p) of the partially cured N-photoPDMS as $D_c = T_l - T_p$. In the experiments, the width of the optical pattern and the initial thickness (T_l) of the spin-coated layer are chosen to 100 µm and 40 µm, respectively. The UV intensity is set to 125 mW/cm^2, and the exposure time ranges from 4 to 30 seconds. One can see that thickness of the cured N-photoPDMS increases with increasing exposure energies and reaches saturation according to Beer-Lambert law.

3.2 Direct fabrication of large-area microfluidic chip with microscale herringbone mixers

To show the large-area patterning capability of the technology, a microfluidic chip with complex staggered herringbone mixers (SHMs) was fabricated in the experiment. The embedded SHMs could enable rapidly mixing in a shorter section, which is desired in many chemical biological applications [23-25]. As the total area of microchannels is typically smaller than other region in large-area microfluidic chips, P-photoPDMS, rather than N-photoPDMS, was chosen to fabricate the microfluidic chip for saving exposure time.

The size of the chip is 5.5 × 2.8 cm^2, whose channel width and height are 400 µm and 30 µm, respectively. The width of the flow-merging region is 2800 µm, in which 7 branching channels merge to generate a concentration-gradient flow. With the own-developed add-on program, the 3D model designed by commercial CAD software, as shown in Fig. 6(a), was firstly sliced into 50~255 layers of images with 15500 × 7392 pixels, where the number of layers were used to control exposure time to generate gray levels. Since the width of a single pixel of the

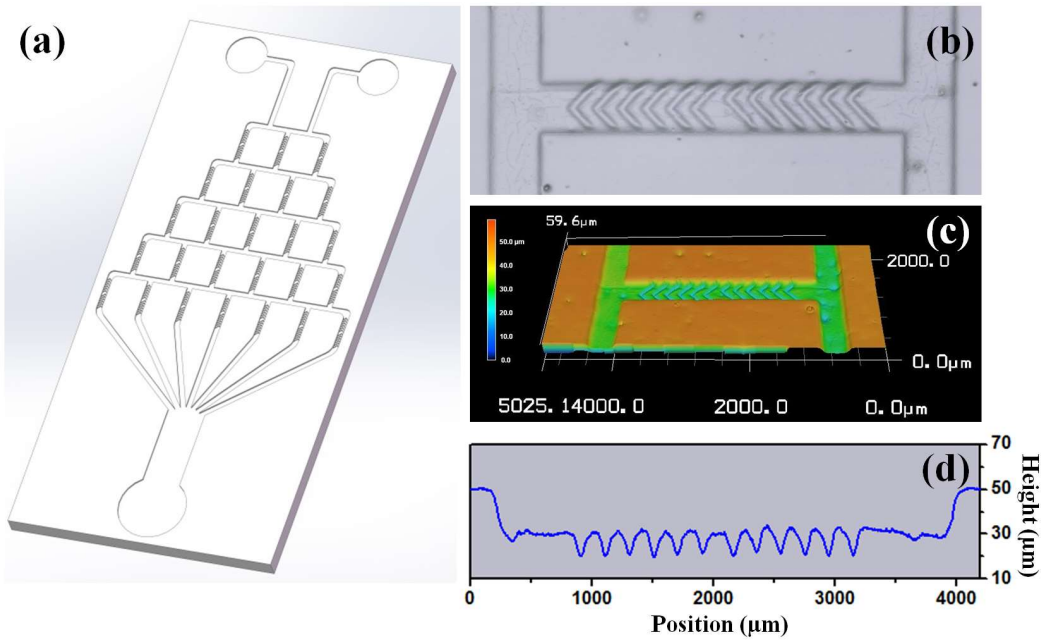

Fig. 6 (a) 3D model of a PDMS microfluidic chip with 5-level gradient generator, (b, c) optical microscope image and laser scanning confocal image of the fabricated staggered herringbone mixer, (d) a cross-section profile of the SHM along the channel axis.

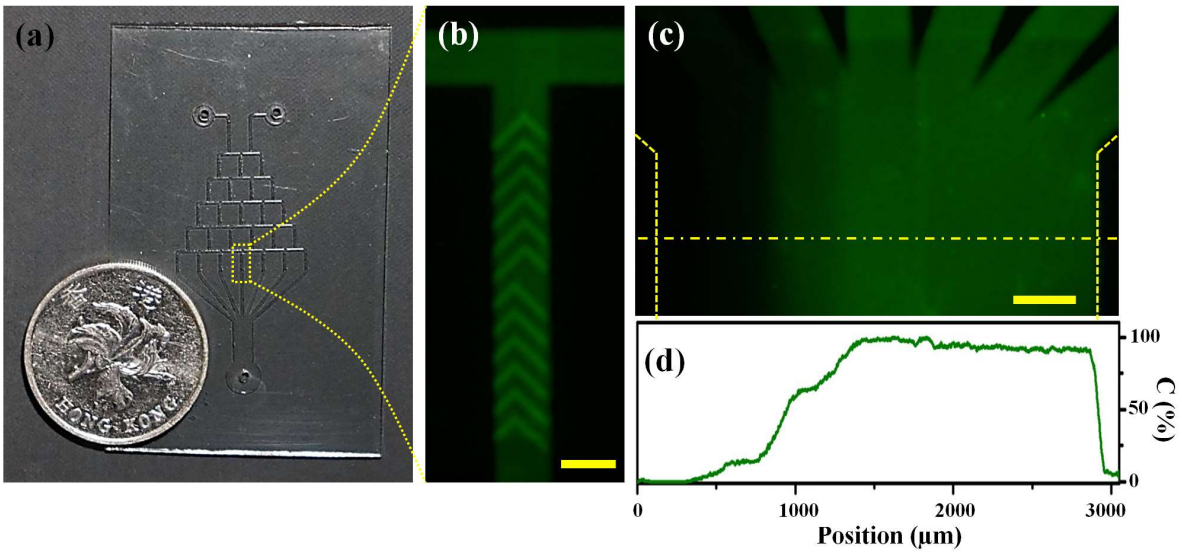

Fig. 7 (a) Photo of the fabricated large-area microfluidic chip with staggered herringbone mixers, (b) fluorescence photograph of the microchannel with SHM structure, (c) fluorescence photograph of the flow-merging region, (d) calculated concentration distribution of the solution across the flow-merging region by using the fluorescence intensity marked with the yellow dot-dashed horizontal line in Fig. 4c. Scale bar: 400 μm.

DMD chip is 13.68 μm and the demagnification factor of 5 is used in the projection optics, the size of each pixel of the optical pattern is around 2.7×2.7 μm^2. Gray levels between 0 and 255 were used to smooth the edges according to the subpixel area of the sliced image. In order to create those SHMs inside microchannels, a specific gray level was properly chosen according to the data given in Fig. 3(c) to generate the bottom of the microchannel and then the SHMs were digitalized among the gray levels between 255 and the gray level for the bottom.

In the experiments, a pre-cured PDMS film with the thickness of 1 mm was used as a substrate. P-photoPDMS was then spin-coated on the substrate for optical exposure process. The thickness of the prepared P-photoPDMS film is around 60 μm. The UV intensity is 330 mW/cm^2, and the exposure time for individual sub-patterns is 60 seconds. The fabricated SHM structures are shown in Fig. 6(b) to (d) by using 3D laser scanning confocal microscope (VK-X200, KEYENCE), while a scanning electron microscope (SEM) image is given in Fig. S2(a). One can see that the embedded staggered herringbones have been successfully fabricated by a single-step exposure process. The cross section of the SHM along the channel axis was measured as shown in Fig. 6(d). The depth of the microchannel was ~ 22 μm, and the depth of SHM grooves are ~10 μm. The profile of the fabricated SHM agrees well with the designed structural parameters.

The fabricated microfluidic chip with SHMs, as shown in Fig. 7(a), was then bonded with a clean glass wafer after O_2 plasma treatment (45 W, 400 mTorr, 3 min). Although photoPDMS includes other ingredients, it can bond well with plasma-treated glass substrate, like conventional PDMS. Fluorescein isothiocynate (FITC) (100 μM FITC in 100 mM $NaHCO_3$ buffer, pH 8.3) and buffer solutions were then injected into the inlets of the chip simultaneously at flow rate of 0.5 μL/min by using two syringes mounted on a motorized syringe pump. Fig. 7(b) shows the fluorescence photograph of FITC solution taken with an inverted microscope (Eclipse TE2000-U, Nikon) when steady flow passes through the SHM region. When the solutions stably flowed through the microchannel, concentration gradient was successfully observed in the flow-merging region, as shown in Fig. 7(c) and (d). The flow speed at the outlet channel was estimated to be 0.3 mm/s. Two parallel dashed lines in Fig. 7(c) indicate the boundaries of the flow-merging region. Fig. 7(d) shows the normalized concentration distribution of the solution across the flow-merging region, which was calculated according to fluorescence intensity of the place marked with the yellow dot-dashed horizontal line in Fig. 7(c). The result is consistent with that in the previous report [23].

3.3 In-situ surface engineering of microchannels for cell migration study

Microfluidic chips have become a promising platform to investigate cell migration behaviours, particular their responses to geometric cues and chemical signals. gDPL technology is able to additively print polymer microstructures on the microchannel to customize microenvironments for cell culture and migration studies.

Here, a special microfluidic chip with two reservoirs and four connecting microchannels, as shown in Fig. 8(a) and (b), are designed and fabricated for the study of the migration behaviour of human mesenchymal cell (hMSCs), which is of interest for injury healing [26, 27]. In particular, microridges with different heights were introduced to the bottom of microchannels to investigate hMSCs' migration behaviours. After preparation of the microchannels with the height of 80 μm and the width of 150 μm with N-photoPDMS, N-photoPDMS solution was dropped and patterned into microridges by using the bottom-up exposure process shown in Fig. 3(d). As shown in Fig. 8(c1) to (c3), the heights of the microridges in four microchannels are 0, 10 μm, 20 μm and 30 μm, respectively. An SEM image of the sample is given in Fig. S2(b). In order to improve cell adhesion, polydopamine has been used to coat the corrugated structures before cell culture[28]. The fabricated PDMS microfluidic chip was immersed into 0.01 %w/v dopamine (Sigma Aldrich) in 10mM Tris-HCl (pH8.5) solution for 24h. The chip was then washed with 1X phosphate buffered saline (PBS) to remove unattached polydopamine molecules, and was sterilized by UV exposure for 1 h before cell culture.

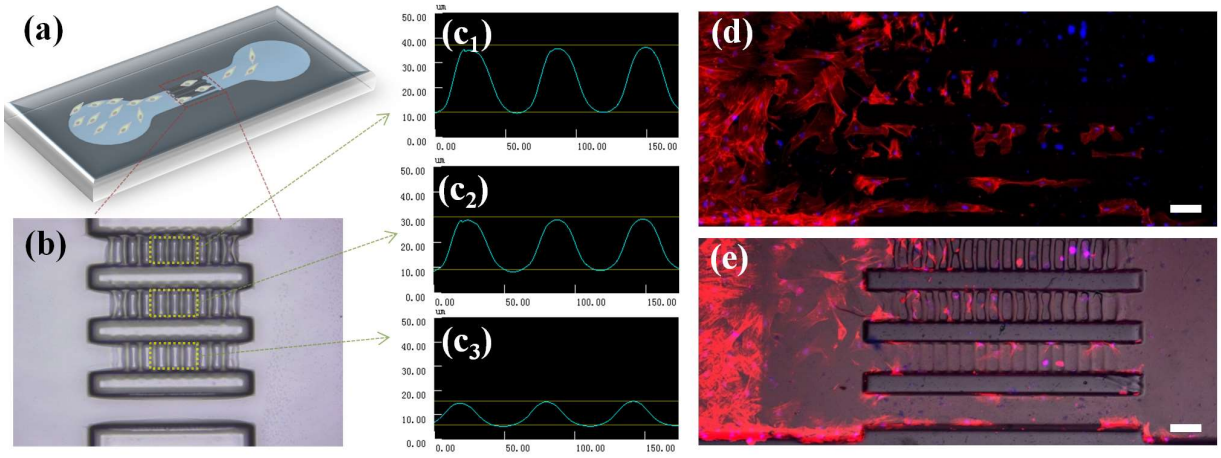

Fig. 8 (a) Schematic design of the microfluidic chip for cell migration study. (b) Microscope image of the microfluidic channels with corrugated microstructures. (d) Fluorescence photograph, (e) merging photograph. hMSCs were stained for actin (red) and DAPI (blue). Scale bar: 100 μm.

The cells were added to and proliferated in one of the reservoirs on the microfluidic chips without use of cover slide. All cell experiments were conducted at 37 °C and 5% CO_2. Human mesenchymal stem cells (hMSCs) (Lonza) were expanded to passage 4 in basal growth medium (GM), i.e., alpha-Minimum Essential Medium supplemented with 16% Fetal Bovine Serum (FBS) (Invitrogen), 1% streptomycin/penicillin(Invitrogen), and 1% L-glutamine(Invitrogen). All chips were put into 6-well plates for cell culture. Around 20000 number of hMSCs concentrated in 15 μl of GM by centrifugation were pipetted onto the entry reservoir of the microfluidic chip surface. The cells were incubated with 3 h to stabilize the cell adhesion. It was followed by addition of 2 ml GM for long-term cell culture and cell migration.

As F-actin is the physical bridge for sensing the mechanical cues [29, 30], the F-actin and nucleus of cells were stained on the sixth day for the cytoskeleton visualization. Cytoskeleton F-actin and nucleus of hMSCs were stained with 1:200 fluorescent phalloidin (Life Technologies) in 0.5% BSA in PBS for 1 h and 1:1000 DAPI in PBS for 20 min, respectively, in dark condition. The overlapping of dapi and F-actin fluorescent are counted as one cell. The photo of the final state of the cells is shown in Fig. 8(d) and (e). From the results, one can see that the cells migrated at the fastest speed on flat surface. With the increment of the heights of the microridges, the migration speeds of cells became lower gradually.

4. Conclusions

A new optical microfabrication technology has been demonstrated to fabricate PDMS microfluidic devices. With positive- and negative-tone photosensitive PDMS, various PDMS microstructures and devices have been successfully fabricated by using either top-down or bottom-up optical maskless exposure techniques. A large-area microfluidic chip with complex staggered herringbone mixers has been fabricated with the positive-tone photosensitive PDMS for microfluidic gradient generation, while a group of microridges of different heights has been *in-situ* printed on the microchannels with negative-tone photosensitive PDMS to for cell migration study. The technology will offer new opportunities for rapid fabrication of novel PDMS microfluidic devices for various kinds of applications ranging from lab-on-a-chip to tissue engineering.

Acknowledgements

The authors would like to thank our colleague, Mr. Mian Yao and Dr. Mingjie Yin for their assistances on the preparation of the negative-tone photosensitive PDMS. This work was partially supported by Hong Kong RGC GRF (Grant No.: PolyU 152211/14E) and PolyU General Research Fund (Grant No.: G-YBLJ and 1-ZVHB).

References

[1] Terry S C, Jerman J H and Angell J B 1979 A gas chromatographic air analyzer fabricated on a silicon wafer *IEEE Transactions on Electron Devices* **26** 1880-6
[2] Manz A, Fettinger J C, Verpoorte E, Lüdi H, Widmer H M and Harrison D J 1991 Micromachining of monocrystalline silicon and glass for chemical analysis systems A look into next century's technology or just a fashionable craze? *TrAC Trends in Analytical Chemistry* **10** 144-9
[3] Waldbaur A, Rapp H, Länge K and Rapp B E 2011 Let there be chip—towards rapid prototyping of microfluidic devices: one-step manufacturing processes *Analytical Methods* **3** 2681-716
[4] McDonald J C and Whitesides G M 2002 Poly(dimethylsiloxane) as a Material for Fabricating Microfluidic Devices *Accounts of Chemical Research* **35** 491-9
[5] Xia Y and Whitesides G M 1998 Soft lithography *Annual Review of Materials Science* **28** 153-84
[6] Qin D, Xia Y and Whitesides G M 2010 Soft lithography for micro- and nanoscale patterning *Nat. Protocols* **5** 491-502
[7] Duffy D C, McDonald J C, Schueller O J A and Whitesides G M 1998 Rapid Prototyping of Microfluidic Systems in Poly(dimethylsiloxane) *Analytical Chemistry* **70** 4974-84
[8] Totsu K, Fujishiro K, Tanaka S and Esashi M 2006 Fabrication of three-dimensional microstructure using maskless gray-scale lithography *Sensors and Actuators A: Physical* **130–131** 387-92
[9] Xiang N, Yi H, Chen K, Wang S and Ni Z 2013 Investigation of the maskless lithography technique for the rapid and cost-effective prototyping of microfluidic devices in laboratories *Journal of Micromechanics and Microengineering* **23** 025016
[10] Ningning L and Zhimin Z 2017 Fabrication of a curved microlens array using double gray-scale digital maskless lithography *Journal of Micromechanics and Microengineering* **27** 035015
[11] Scharnweber T, Truckenmuller R, Schneider A M, Welle A, Reinhardt M and Giselbrecht S 2011 Rapid prototyping of microstructures in polydimethylsiloxane (PDMS) by direct UV-lithography *Lab on a Chip* **11** 1368-71
[12] Bhagat A A S, Jothimuthu P and Papautsky I 2007 Photodefinable polydimethylsiloxane (PDMS) for rapid lab-on-a-chip prototyping *Lab on a Chip* **7** 1192-7
[13] Martínez Rivas A, Suhard S, Mauzac M, Mingotaud A-F, Séverac C, Collin D, Martinoty P and Vieu C 2010 Simplified and direct microchannels fabrication at wafer scale with negative and positive photopolymerizable polydimethylsiloxanes *Microfluid Nanofluid* **9** 439-46
[14] Choi K M and Rogers J A 2003 A Photocurable Poly(dimethylsiloxane) Chemistry Designed for Soft Lithographic Molding and Printing in the Nanometer Regime *Journal of the American Chemical Society* **125** 4060-1
[15] Tsougeni K, Tserepi A and Gogolides E 2007 Photosensitive poly(dimethylsiloxane) materials for microfluidic applications *Microelectronic Engineering* **84** 1104-8
[16] Lu D-X, Zhang Y-L, Han D-D, Wang H, Xia H, Chen Q-D, Ding H and Sun H-B 2015 Solvent-tunable PDMS microlens fabricated by femtosecond laser direct writing *Journal of Materials Chemistry C* **3** 1751-6

[17] Femmer T, Kuehne A J C and Wessling M 2014 Print your own membrane: direct rapid prototyping of polydimethylsiloxane *Lab on a Chip* **14** 2610-3
[18] Zhang A P, Qu X, Soman P, Hribar K C, Lee J W, Chen S and He S 2012 Rapid Fabrication of Complex 3D Extracellular Microenvironments by Dynamic Optical Projection Stereolithography *Advanced Materials* **24** 4266-70
[19] Yin M-J, Yao M, Gao S, Zhang A P, Tam H-Y and Wai P-K A 2016 Rapid 3D Patterning of Poly(acrylic acid) Ionic Hydrogel for Miniature pH Sensors *Advanced Materials* **28** 1394-9
[20] Wu J, Guo X, Zhang A P and Tam H-Y 2015 Rapid 3D µ-printing of polymer optical whispering-gallery mode resonators *Opt. Express* **23** 29708-14
[21] Seo J, Lean M H and Kole A 2007 Membrane-free microfiltration by asymmetric inertial migration *Applied Physics Letters* **91** 033901
[22] Yang J, Qi L, Chen Y and Ma H 2013 Design and Fabrication of a Three Dimensional Spiral Micromixer *Chinese Journal of Chemistry* **31** 209-14
[23] Jeon N L, Dertinger S K W, Chiu D T, Choi I S, Stroock A D and Whitesides G M 2000 Generation of Solution and Surface Gradients Using Microfluidic Systems *Langmuir* **16** 8311-6
[24] Dertinger S K W, Chiu D T, Jeon N L and Whitesides G M 2001 Generation of Gradients Having Complex Shapes Using Microfluidic Networks *Analytical Chemistry* **73** 1240-6
[25] Campbell K and Groisman A 2007 Generation of complex concentration profiles in microchannels in a logarithmically small number of steps *Lab on a Chip* **7** 264-72
[26] Ji J F, He B P, Dheen S T and Tay S S W 2004 Interactions of Chemokines and Chemokine Receptors Mediate the Migration of Mesenchymal Stem Cells to the Impaired Site in the Brain After Hypoglossal Nerve Injury *STEM CELLS* **22** 415-27
[27] Humphreys B D and Bonventre J V 2008 Mesenchymal Stem Cells in Acute Kidney Injury *Annual Review of Medicine* **59** 311-25
[28] Chuah Y J, Koh Y T, Lim K, Menon N V, Wu Y and Kang Y 2015 Simple surface engineering of polydimethylsiloxane with polydopamine for stabilized mesenchymal stem cell adhesion and multipotency *Scientific Reports* **5** 18162
[29] Geiger B, Bershadsky A, Pankov R and Yamada K M 2001 Transmembrane crosstalk between the extracellular matrix and the cytoskeleton *Nat Rev Mol Cell Biol* **2** 793-805
[30] Kushiro K, Sakai T and Takai M 2015 Slope-Dependent Cell Motility Enhancements at the Walls of PEG-Hydrogel Microgroove Structures *Langmuir* **31** 10215-22